Thermal Hydraulic Design Aspects of an Integral Pressurized Water Reactor

VINCENZO ZINGALES
Nuclear Research Group of San Piero a Grado, (University of Pisa, UNIPI)
Largo Lucio Lazzarino, 1, Pisa, Italy
Department of Nuclear Engineering, (Texas A&M University)
3380 University Drive E, College Station, Texas, USA
vincenzo.zingales21@gmail.com

FRANCESCO S. D'AURIA
Nuclear Research Group of San Piero a Grado, (University of Pisa, UNIPI)
Largo Lucio Lazzarino, 1, Pisa, Italy
francesco.saverio.dauria@unipi.it

YASSIN A. HASSAN
Department of Nuclear Engineering, (Texas A&M University)
3380 University Drive E, College Station, Texas, USA
y-hassan@tamu.edu

ABSTRACT

This work presents a customized RELAP5-3D nodalization designed specifically for an iPWR (integral Pressurized Water Reactor) operating under natural circulation conditions. Given the absence of appropriate correlations in the used SYS-TH (system-thermal hydraulic) code for HCSGs (Helical Coil Steam Generators), tuning of pressure drops and HTC (Heat Transfer Coefficient) has been necessary on both sides of these heat exchangers.

Following the successful simulation of steady state conditions at full power, a comprehensive start-up procedure has been implemented, comprising power increase ramps and steady-state assessments. During these simulations, DWOs (Density Wave Oscillations) in the secondary side at low power conditions have been encountered, prompting exploration of mitigation strategies leveraging the understanding of Ishii-Zuber dimensionless numbers, namely the Phase Change Number and the Subcooling Number.

Thereafter, a power uprate under primary forced circulation is pursued. The integrated linear heat generation rate of the hottest rod is increased to 55 kW/m, followed by the scaling of the reactor power accordingly. The angular speed of the implemented primary pumps is regulated using an integral controller. Results indicate reasonable superheating in the secondary side and satisfactory subcooling at the core outlet. Given the reactor's small core dimensions and the significant power increase achieved, fuel cycle duration would be substantially shortened unless fuel enrichment is increased.

Keywords: *iPWR, SMR, RELAP5-3D, natural circulation, DWOs, HCSGs*

1 INTRODUCTION

1.1 Small Modular Reactors

In recent years, the imperative for decarbonization and achieving energy independence has become increasingly pressing. Nuclear power clearly stands out as a pivotal player in addressing these challenges. However, the landscape of large-scale nuclear power plants in many Western economies has been marred by cost overruns and a lack of political will to pursue a renaissance in this sector. Private investors are often inclined towards renewable technologies due to subsidies and the relatively rapid return on investment they provide. However, it is widely acknowledged that in an electrical grid, baseload energy sources play a crucial role in its stability, a requirement that intermittent renewables are unable to meet, especially considering the limitations of current energy storage technologies, which are generally incompatible with seasonal electricity storage.

Consequently, there has been a growing interest in the concept of leveraging mass production in the nuclear power sector, with a focus on small-scale, factory-built reactors. This approach promises expedited construction schedules and reduces initial capital outlay, while giving the possibility to account for baseload energy production. It's worth noting that the decision to increase the size of nuclear reactors 60-70 years ago was primarily driven by economic factors, namely economies of scale and neutron economics. Only time will reveal which scale choice proves more advantageous. Still, SMRs (Small Modular Reactors) could offer unquestionable deployment opportunities concerning the installation in remote locations and regions with small energy grids. However, this study does not primarily focus on the economic aspects of SMRs, but rather on some design characteristics of one of the most promising types. Among SMRs, being reactors with a power output up to 300MWe, the water-cooled, water-moderated types, drawing upon almost 20,000 years of LWRs (Light Water Reactors) operational experience, are the closest to realization. In this study, emphasis has been placed on the iPWR type. [1] [2]

1.2 Integral Pressurized Water Reactors

iPWRs are essentially water cooled, water moderated pressurized water reactors. This means that the water within the reactor core remains in a liquid state (except for some eventual subcooled nucleate boiling), and heat is transferred to the secondary side through heat exchangers, known as steam generators. The fuel enrichment is typically lower than 5%. Operating conditions in iPWRs closely resemble those of traditional PWRs (Pressurized Water Reactors), particularly in terms of primary pressure, which is typically maintained at or below 15.5 MPa to ensure a certain degree of subcooling at the core exit. Because of the reduced core dimensions, the conventional enrichment, and the necessity to have a reasonably long fuel cycle, the linear heat generation rate and the core power density are smaller than the one achieved in large PWRs.

The predominant flow trajectory of the primary reactor coolant involves an ascent from the core through the central hot leg riser, followed by a descent along the exterior of the HCSGs tubes, with the return flow directed towards the base of the core via an annular DC (Downcomer). During this transit across the SGs tubes, heat is transferred to the secondary side water contained within the tubes. Simultaneously, the secondary side fluid undergoes a progression upwards within the SGs tubes, where it experiences heating, vaporization, and subsequent superheating, culminating in the generation of high-pressure steam intended for the turbine generator unit.

A notable departure from traditional PWRs, besides their size, is the internal positioning of SGs within the reactor vessel, specifically located in the downcomer region. Unlike conventional PWRs, iPWRs adopt OTSGs (Once-Through Steam Generators), obviating the necessity for steam separators and dryers, thereby simplifying the design. To augment heat transfer efficiency, iPWRs integrate HCSGs, thereby amplifying both the heat transfer area per unit volume and the HTC. Within these systems, the secondary flow ascends within the tubes, while the primary flow operates in a counter-current fashion.

In contrast to U-tube steam generators, OTSGs generally afford a much briefer grace period in the event of feedwater loss, as exemplified by the TMI2 accident. However, iPWRs frequently offset this reduction in secondary water volume by augmenting the primary volume (relative to core power), and by featuring a design characterized on the availability of emergency heat exchangers immersed in large water pools for decay heat dissipation. Additionally, OTSGs, due to their modest water inventory, mitigate the potential for a return to power subsequent to a steam line break accident. The thermodynamic cycle employed is a Rankine-subcritical regenerative cycle with superheat.

A significant simplification and safety enhancement is achieved by eliminating external piping, thereby eliminating by design the risk of LBLOCAs (Large Break Loss Of Coolant Accidents), which are among the most challenging scenarios to manage.

Primary coolant circulation in iPWRs can be achieved through either natural or forced circulation. Natural circulation necessitates a substantial elevation difference between core and steam generators, requiring taller vessel structures and containment systems. In contrast, forced circulation systems require specialized pumps to induce circulation, adding maintenance requirements and additional capital costs. However, pump-assisted circulation offers the potential to increase the primary flow rate, thereby safely enhancing core power output without inducing DNB (Departure from Nucleate Boiling). Additionally, pumps can help prevent flow oscillations in the primary side.

Moreover, iPWRs frequently incorporate a substantial pressurizer volume relative to power output, ensuring a significant margin for power adjustments. A considerable volume of primary coolant affords substantial thermal inertia and prolonged response times, thereby fortifying resilience against some kinds of operational transients and design basis accidents.

Also, they often depend on passive safety systems to manage design basis events. Proponents of such solutions argue for enhanced safety, implying a reduced core damage frequency. However, according to some experts, this assertion requires substantiation and may not necessarily hold true. Nonetheless, it is indisputable that these systems offer cost-effective alternatives to their active counterparts in terms of construction and maintenance. [3]

Several iPWR designs have been developed, each possessing distinct characteristics and operational parameters. [4,14]

2 DESCRIPTION OF THE REFERENCE I-PWR DESIGN

2.1 Background and history

The reference design is vaguely inspired to the NuScale design [14] even though this study does not claim to mirror the NPM (NuScale Power Module) normal operation characteristics nor its response to operational transients or accidental conditions. Anyway, in the following a description of the NuScale design itself will be given.

The NuScale SMR has been developed based on the expertise acquired from the MASLWR facility, initiated at the beginning of the millennium. This facility, spearheaded by OSU (Oregon State University) and funded by the U.S. Department of Energy, laid the foundation for the NuScale reactor. The OSU-MASLWR facility is characterized by a 1:3 length scale, 1:254.7 volume scale, and 1:1 time scale compared to the originally planned full-scale MASLWR reactor prototype. The transition of OSU patents to NuScale in 2007 led to the establishment of the company.

NuScale achieved a significant milestone in 2020 by obtaining NRC approval for its SMR design. This approval allows for a configuration accommodating up to 12 modules, each capable of generating 50 MWe of power. Subsequently, in March 2023, NuScale submitted an application to the NRC for its plant design featuring upgraded 77 MWe NPMs. The project was close to deployment at the UAMPS Carbon Free Power Project, sited at the Idaho National Laboratory, but

it faced cancellation in November 2023 due to projected cost escalations and challenges in garnering unanimous municipal support.

2.2 Technical characteristics

The design of the NuScale reactor [14] features an integral power module housing the reactor core, two helical coil steam generators, and a pressurizer within the reactor vessel. The RPV (Reactor Pressure Vessel) is enveloped by a CNV (Containment Vessel), partially submerged in a pool serving as the ultimate heat sink for long-term decay heat removal. The primary system flow is driven by natural circulation. Safety systems are fully passive obviating the need for emergency diesel generators.

Leveraging reduced source term characteristics compared to large LWRs, NuScale secured NRC (Nuclear Regulatory Commission) approval for an EPZ (Emergency Planning Zone) confined to the site boundary, in contrast to the conventional 10-mile (16km) radius zone mandated for standard nuclear power plants in USA.

The reactor pressure vessel is a cylindrical steel vessel with an inside diameter of approximately 3m and an overall height of approximately 18m, designed to withstand an operating pressure of approximately 12.8 MPa. A flanged lower portion facilitates refueling access.

The reactor's pressurizer system maintains coolant pressure through a pair of heater bundles installed above the pressurizer baffle plate and a spray provided by the chemical and volume control system. A steel pressurizer baffle plate integral with the RPV provides a barrier between the saturated water in the pressurizer and the RCS (Reactor Coolant System). The pressurizer baffle plate is integrated with the upper steam plenums, has 8 flow holes having a 10cm diameter each to allow surges of water into and out of the pressurizer, and to act as a thermal barrier.

The core configuration for the NPM consists of 37 fuel assemblies and 16 CRAs (Control Rod Assemblies).

The fuel assembly design is like a standard 17x17 PWR fuel assembly. The only significant differences are that the fuel assembly is nominally half the height of a standard fuel assembly and is supported by five spacer grids. The fuel is uranium dioxide, with gadolinium oxide as a burnable absorber homogeneously mixed within the fuel in select rods. The U-235 enrichment is less than 4.95 percent. A seamless M5R fuel rod cladding encapsulates the fuel pellets which are cylindrically shaped with a spherical dish and chamfer at each end. Each fuel rod has an internal spring system which axially restricts the position of the fuel stack within the rod. The fuel rods are pressurized with helium.

The CRAs are organized into two banks: a regulating bank and a shutdown bank. The regulating bank is used during normal plant operation to control reactivity. The shutdown bank is used during normal shutdown. All 16 CRAs are inserted for scram events. The individual rods contain B4C pellets in the upper portion of the rod, and AIC absorber in the tip of the rod. This hybrid configuration of AIC and B4C is adapted to the NuScale design to reduce the total weight of the CRAs (B4C is lighter than AIC).

Unlike the AIC material, the B4C can produce helium gas under neutron fluence leading to the potential buildup of gas pressure in the rod. Thus, the use of B4C is restricted to the low flux region at the top of the rod where helium production is minimal, and the AIC material is used in the high flux region. The rod internals are sealed within a 304 stainless steel cladding tube to protect the absorber from the coolant. The tube is plugged and welded at each end.

The core is surrounded by a stainless-steel heavy neutron reflector.

Differently from most of the other iPWR designs having many small HCSGs, NuScale features two large HCSGs whose helix is intertwined along the riser assembly axis. This allows symmetrical inlet core temperature even in the case in which only one of them is operating. They are composed by 1380 tubes in total with an average length of about 24m, and an inner diameter of about 1.3cm. Each SG tube is comprised of a helix with bends at each end that transition from the helix to a straight configuration at the entry to the tubes' sheets. In normal operation they produce steam at

3.5MPa, 580K with a moisture content smaller than 0.1 percent. The feed and steam plena comprising a single SG are configured 180 degrees apart and a total of four feed and four steam plena are located 90 degrees apart around the RPV. [11] [12] [13] [14]

3 RELAP5-3D NODALIZATION FOR THE REFERENCE DESIGN

3.1 General guidelines

The general guidelines for setting up the nodalization have been derived from the RELAP5-3D code manuals. [15,16]

As a general rule of thumb in the primary system nodalization, volumes lengths have been kept between 10 and 50cm, mainly around 20cm for the primary circuit but their length can reach 2m in the steam line region. Also, it has been tried, when possible, to keep the ratio length/hydraulic diameter greater than 1 and homogeneous for the system. In fact, having all the nodes with the same Courant limit, would allow the selection of an optimized maximum time step, beneficial both from the point of view of computational time and numerical accuracy.

In the primary system, as well as in all the natural circulation loops modeled in this work, the "slice nodalization" technique is implemented to enhance the code's ability to replicate natural circulation phenomena. This approach involves dividing mesh cells into different nodalization zones at the same elevation, each with identical cell lengths. By doing so, errors stemming from the position or elevation of the cell nodalization center, which could impact calculated data accuracy, particularly in the presence of natural circulation regimes, are mitigated. These errors stem from the computation of the gravitational contribution to the momentum equation of physically parallel volumes situated at points with varying elevations. Consequently, they aggregate to form a kind of spurious pump effect. Without employing the "slice nodalization" technique, these errors must be considered, especially as they amplify with the use of larger nodalization cells. However, employing a "fine nodalization" can alleviate this issue. While the impact of this error on results is generally less significant in simulations of forced circulation regimes, adopting the "slice nodalization" technique may necessitate nodes of smaller lengths, potentially leading to increased numerical errors and computational time. [17] This is for instance true in the present work, where the part of downcomer parallel to the core, is characterized by relatively short nodes.

All the major flow paths have been represented: the main flow path (core, riser, downcomer, lower plenum), the guide tube bypass, the reflector bypass, and the connection between the downcomer and the pressurizer through the pressurizer plate.

A flow path was disregarded due to insufficient information and its insignificance to the conducted simulations. In the reference design, certain holes establish connections between the riser region and the steam generator region. In this configuration, if the water level were to decrease below the riser height and unborated steam were to condense in the downcomer, these holes would facilitate the mixing of borated water from the riser with the condensate entering the downcomer. This mechanism serves to prevent undesired reactivity injection when the condensate reaches the core.

Throughout the nodalization, the default format for junctions and volumes flags has been adhered to. However, a departure from this convention is observed in both the downcomer-steam generator region and the core, where, in the volume control flags, the option b=1, has been selected. This option allows the use of the rod bundle interphase friction model. Although the DC-SG region is not properly having vertical bundles in it, using the option b=1 is clearly more accurate than using the pipe interphase friction model.

3.2 Core

The core is represented by a single hydraulic channel (pipe component) in which five heat structures levels are located. In particular, the core fuel assemblies have been thermally divided into three radial regions: the peripheral, the intermediate and the inner region. In addition, the hot fuel assembly and the hot rod are individually represented as well. The core power is divided into these structures referring to the beginning of cycle, equilibrium cycle, axial and radial distributions. The utilized fuel rods length keeps into account thermal expansion. In particular, the full power steady state volumetric average temperature of the fuel has been used, in combination with an appropriate volumetric expansion coefficient, to get the hot rods average length.

3.3 Downcomer (Steam generator region)

In RELAP5-3D, correlation for flow across a tube bank are not available: that's true for both friction and heat transfer aspects. The downcomer hydraulic diameter has been reduced with respect to the estimated tubes distance in order to increase the pressure drops. To increase the HTC of the shell side of the heat exchanger a reduction of the heated diameter has been implemented.

3.4 Primary system's pressure drops

To adjust the core and bypass flow rates within the primary circuitry, a decision was made to simply reduce the HD (Hydraulic diameter) in specific areas, being the downcomer (in the steam generator region), the guide tubes, and the reflector holes. This adjustment strategy was chosen over employing arbitrary localized singular pressure drop coefficients in the primary side, shifting the responsibility of tuning the primary flow to the downcomer itself. Consequently, a substantial reduction of the physical hydraulic diameter was deemed necessary. Singular pressure drops coefficients have only been used at spacer grids' locations.

3.5 HCSGs

The 1380 helical tubes of the reference iPWR are divided into four groups and are connected to the four feedwater headers and four steam plena.
In the RELAP5-3D nodalization, each one of these four groups of tubes is modeled by a single pipe. Each pipe is characterized by an equivalent flow area, an average length, an estimated pitch angle and a hydraulic diameter equal to the geometric one. In this phase, it was deemed not necessary a reduction of the HD in the tubes because of the arbitrarity of the singular pressure drop at the tubes inlet.
At each tube inlet, a flow restrictor is present in order to increase pressure drops and to avoid DWOs for full power conditions. To simulate this feature, an arbitrarily large k-factor has been placed at the inlet junction of each of the tubes.
The heated diameter has been reduced to increase the HTC. It has been checked that the order of magnitude of the HTC is the same as the one provided by correlations available in literature. [18,29]

3.6 Nodalization sketches

A sketch of the primary side nodalization is shown in Figure 1., while a sketch of the nodalization adopted for the secondary side is shown in Figure 2.

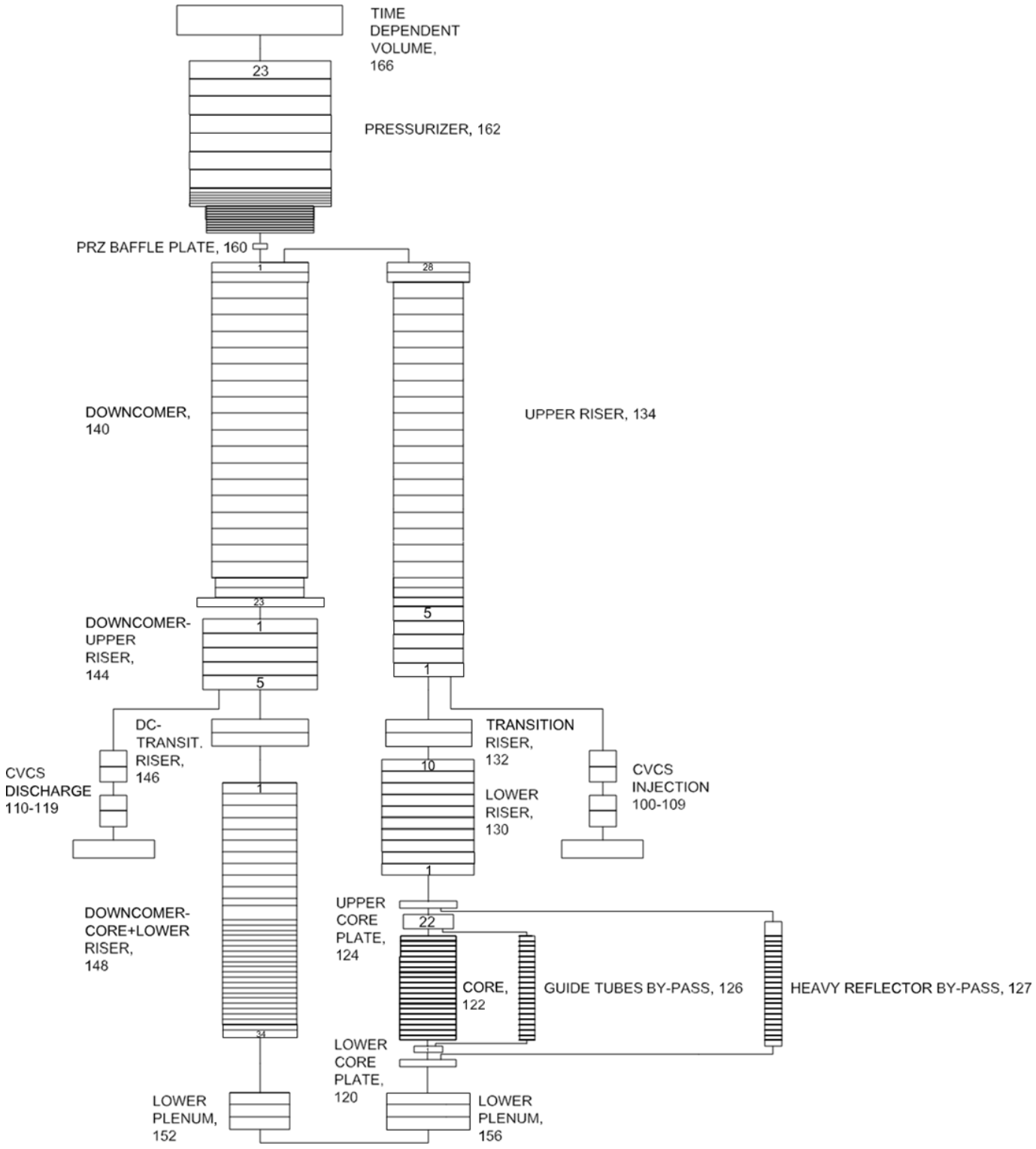

Figure 1. Primary side nodalization

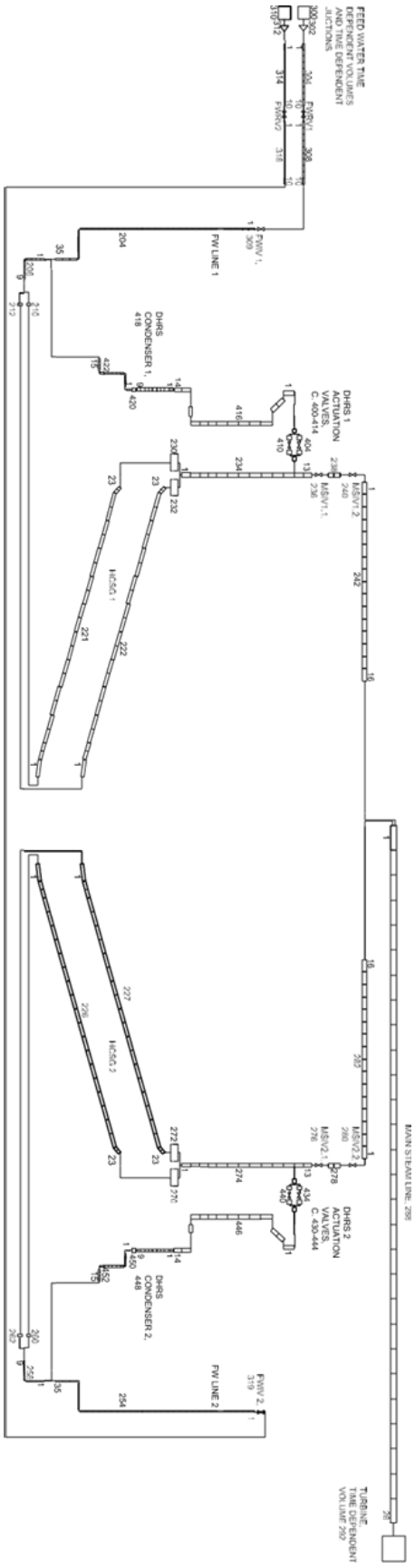

Figure 2. Secondary side nodalization

3.7 Steady state results

In Table 1., a comparison between some relevant parameters as reported in the reference documentation [14], and the data obtained by using RELAP5-3D is presented.

Table 1. Steady state in natural circulation: main parameters comparison

Parameter (unit)	Reference [14]	RELAP5-3D
Core thermal power (MW)	160	160
Average linear power density (kW/m)	8.2	8.2
Primary pressure (MPa)	12.755	12.755
Primary flow rate (kg/s)	587	586
Bypass flow (%)	7.3	7.2
T cold primary (˚ C)	258	260
T hot primary (˚ C)	314	313
T average primary (˚ C)	284	286
Core delta T (˚ C)	56	53
Subcooling at core outlet (˚ C)	16	17
Secondary flow rate (kg/s)	67	67
SG inlet temperature (˚ C)	149	149
SG outlet temperature (˚ C)	307	311
SG outlet pressure (bar)	34.5	34.5
SG outlet superheat (˚ C)	65	69

4 START-UP IN NATURAL CIRCULATION

4.1 Introduction

An iPWR lacking primary pumps is typically equipped with auxiliary systems designed to elevate the primary water temperature close to the nominal average temperature, primarily for reactivity considerations. In fact, the doppler effect is more efficient at higher fuel temperatures. This is often achieved through the utilization of an external heat source. Furthermore, in the initial stages of the start-up, it is common practice for the pressurizer to be pressurized using nitrogen. Subsequently, this nitrogen is purged through a dedicated line, once saturation conditions are attained in the pressurizer heater bundles region.

These phases are not considered in the present work, and we will commence the procedure after the initial phase, specifically from a steady state performed at 15% power, supposing the pressurizer at the nominal pressure.

To prevent any potential feedback between an arbitrarily set up control system and potential instabilities in the secondary side, the flow rate was manually regulated through an iterative procedure. Specifically, thermodynamic properties tables of water were utilized to adjust the secondary flow rate iteratively though an energy balance, ensuring alignment with the desired primary average temperature. The procedure was iterative both because of the dependence of the HCSGs outlet pressure on the secondary flow rate and because of the interdependence of primary flow (and primary average temperature) on the water density profile in the downcomer and in the core.

Three sets (1.1, 1.2, 2.1, 2.2, 3.1, 3.2) of sensitivity studies were conducted following this procedure. In response to observed instabilities, adjustments were made in the second study of each set. Specifically, singular pressure drops at the inlet of the HCSGs were increased. This modification was implemented based on the understanding that heightened pressure drops at the HCSGs inlet are anticipated to exert stabilizing effects on DWOs. In studies x.1, a k-loss coefficient of the order of 10^3, consistent with the value utilized for the full power steady state, was applied at the inlet of the HCSGs tubes. However, in studies x.2, this coefficient was increased to 10^6. It's important to note that values higher than 10^6 were deemed impractical due to pressure spikes at the steam generator inlet. Such spikes lead to the failure of the code's capability to perform consistent interpolations for thermodynamic properties.

For cases 1.1, 1.2, 2.1 and 2.2, upon reaching this steady state at 15% power, gradual power ramps ensued, with increments of 5% of nominal power occurring over a period of 5’000 seconds. Subsequently, the core power and secondary flow rate were maintained at constant levels for 10’000 seconds, allowing the attainment of a steady state at reduced power. This iterative process continued until the system reached 100% of the nominal power, followed by other 10’000s of constant boundary conditions.

For cases 3.1 and 3.2 instead, being the response of the system faster, the power ramps occurred over a 2’000s period after which core power and secondary flow were held constant for 3’000s. The only exception is the stabilization at 60% power, which was given 20’000s to happen.

4.2 Cases 1.1 and 1.2

In the first two studies, the turbine inlet pressure was maintained at a constant level, consistent with the value employed for the 100% power steady state.

Throughout each power ramp, the feedwater temperature experienced a linear increase starting from 75% of the nominal temperature (measured in Celsius). This progressive adjustment aimed to ensure that by the conclusion of the final ramp, the feedwater temperature matched that utilized for the full power steady state. This adjustment aimed to reflect typical considerations in the balance of plant for regenerative Rankine cycles. To provide context, steam extracted from the turbine is utilized to preheat the feedwater. This practice reduces the fraction of core power required to bring the feedwater to the desired conditions and minimizes heat rejection at the condenser. At lower power conditions, the feedwater preheating is typically less pronounced, as the plant is optimized to operate at maximum efficiency during nominal power operation.

The feedwater flow rate was regulated to uphold a constant primary average temperature throughout the entire process. However, without the implementation of a control system, small deviations from the desired temperature were observed. Essentially, variations in secondary side pressure drops, driven by changes in secondary flow rate, posed challenges in achieving precise tuning. This difficulty was compounded by the fact that the outlet enthalpy of the steam generators is contingent upon pressure. Additionally, primary flow and temperature are influenced by heat transfer dynamics and temperature profiles within the HCSGs. As a result, as already mentioned, slight deviations of a few degrees between the desired and achieved primary temperatures were observed.

The results have indicated significant secondary side oscillations occurring below 60% power in both cases, as shown in Figure 3., despite the implementation of higher singular pressure drop

coefficients in the second study, which were able to mitigate their magnitude to some extent. These oscillations induced fluctuation in the primary flow as well, albeit with significantly smaller magnitude. Moreover, potential neutronic-thermal hydraulic feedback in the primary side were disregarded, as the core power was imposed using a predetermined power versus time table.

The secondary oscillations are predicted by the code as a physical phenomenon (not numerical). As an example, at 30% power, the oscillations period (around 8s), as shown in Figure 4. and Figure 5., is greater than the time step (0.01s). Moreover, the period is comparable with the transit time of the fluid in the HCSGs tubes (about 7s), which has been computed by dividing the tubes length by the average velocity of the fluid. Also, as shown again in Figure 4. and Figure 5., a parallel channel behaviour is predicted. In Figure 6. instead, we can see the propagation of the density wave (or void wave) along one group of tubes, typical of DWOs.

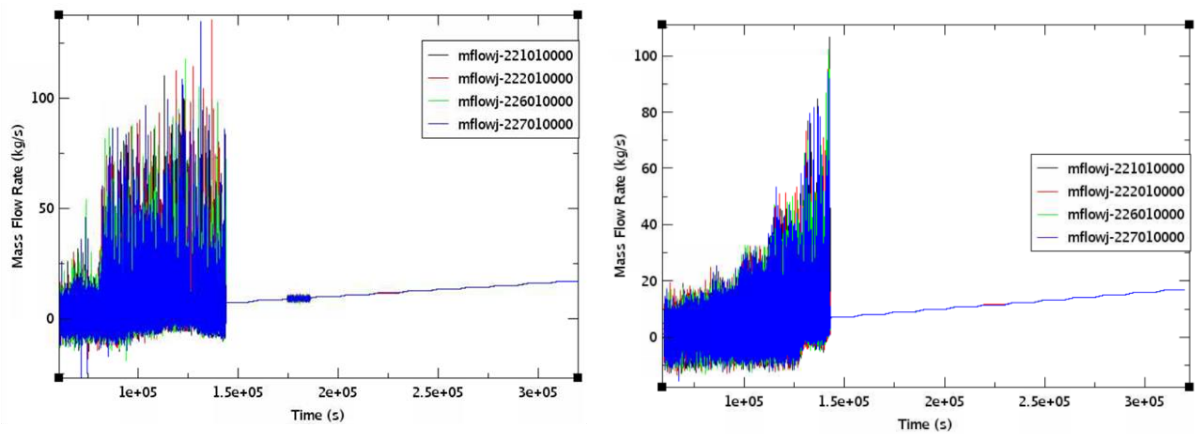

Figure 3. Mass flow rate in each group of steam generator tubes at different power levels in cases 1.1 and 1.2 (Sensitivity to the inlet singular pressure drops)

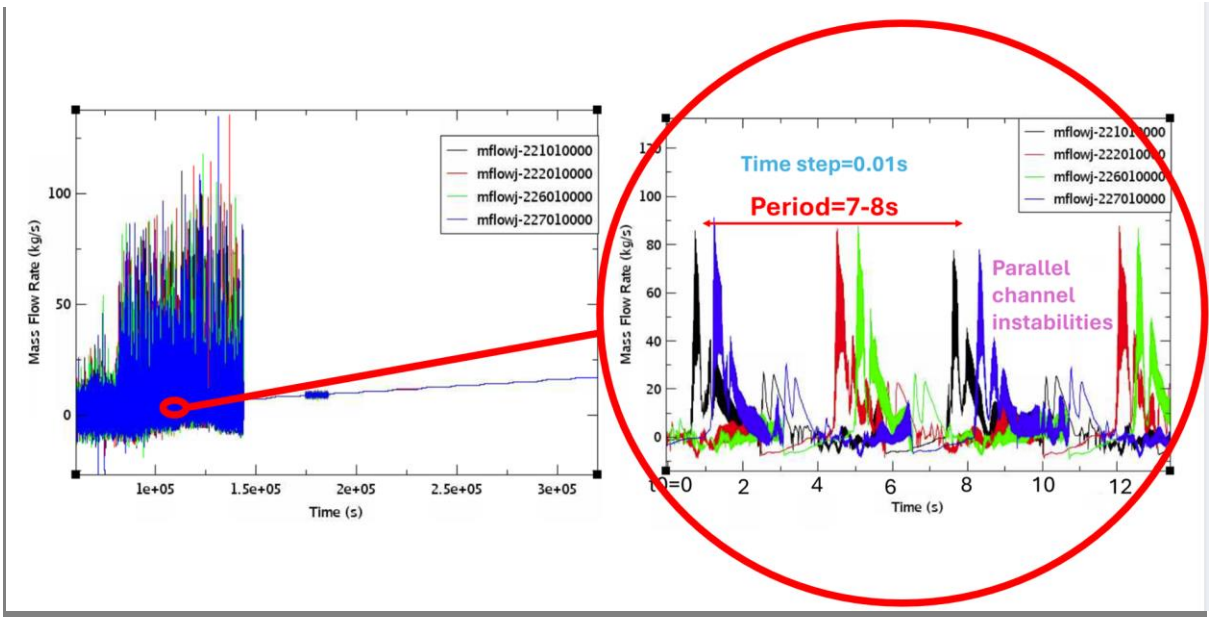

Figure 4. Mass flow rate in each group of steam generator tubes at different power levels in case 1.1 on the left, zoom on the flow rate oscillations at 30% power on the right: the oscillations period is highlighted.

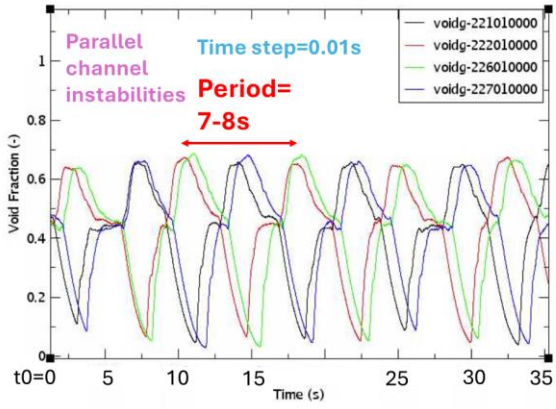

Figure 5. Void fraction in the first volume of each group of steam generator tubes at 30% power for case 1.1. The oscillations period and the parallel channel instabilities can be observed.

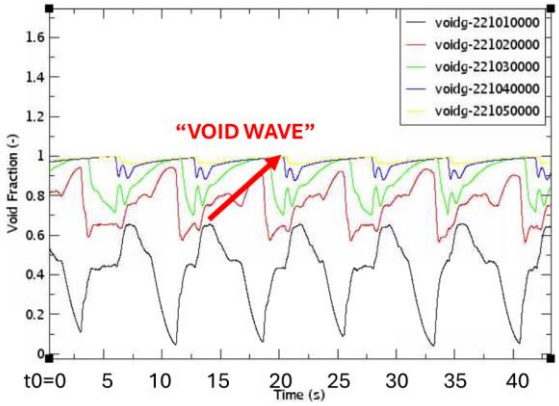

Figure 6. Void fraction in the first five volumes of the first group of steam generator tubes. The density (or void) propagation wave can be noticed.

4.3 Cases 2.1 and 2.2

In these studies, an effort to enhance the feedwater subcooling at low power was undertaken with the intention of reducing the magnitude of density wave oscillations through an increase in the "Subcooling Number" as represented on the Ishii-Zuber plane [30]. To achieve this, the initial turbine inlet pressure was elevated by 45% compared to the nominal value (in bar), and subsequently decreased linearly during each power ramp until reaching the nominal value for full power conditions.

As for the other boundary conditions in cases 2.1 and 2.2, they mirrored the considerations applied in cases 1.1 and 1.2, respectively.

The results of these studies revealed again instabilities occurring below 60% power, analogous to those observed in case 1, but their magnitude is now considerably reduced. In Figure 7. the secondary mass flow rate for each of the four group of SG tubes in case 2.1 and 2.2 is shown.

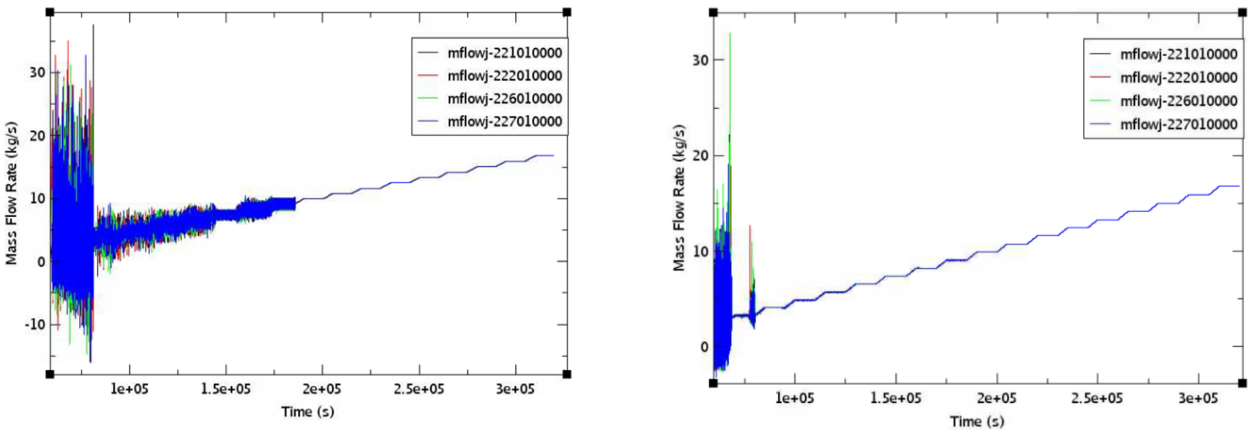

Figure 7. Mass flow rate in each group of steam generator tubes at different power levels in cases 2.1 and 2.2 (sensitivity to the inlet singular pressure drops)

4.4 Cases 3.1 and 3.2

In this last couple of studies, another approach was adopted to address the instabilities experienced up to 55% power. It was decided to increase the secondary flow rate up to the power range characterized by instabilities, ensuring that saturated steam was obtained at the steam generator outlet. This strategy was aimed at reducing the "Phase-Change number" as depicted on the Ishii-Zuber plane [30], thereby exerting a stabilizing effect.

As a consequence of this adjustment, the primary average temperature remained notably below the previously targeted average one, before experiencing a sharp increase once adequate superheating in the secondary side was restored. Through this procedure, significant mitigation of secondary instabilities was achieved. In Figure 8. the secondary mass flow rate for each of the four group of SG tubes in case 3.1 and 3.2 is shown.

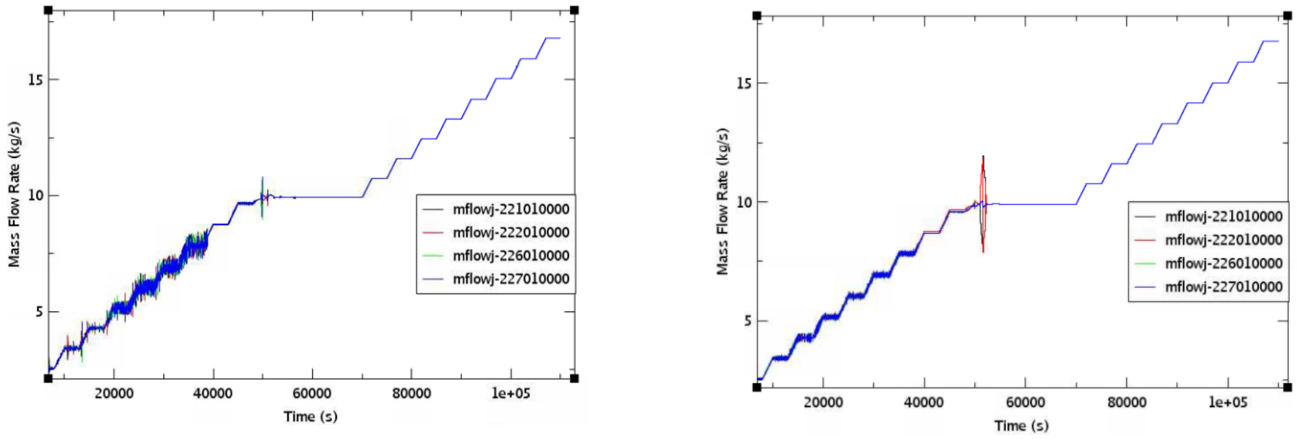

Figure 8. Mass flow rate in each group of steam generator tubes at different power levels in cases 3.1 and 3.2 (sensitivity to the inlet singular pressure drops)

4.5 Final considerations

It should be noted that the absence of correlation for pressure drops in the HCSGs in our model had a stabilizing effect. This was because the simulated distributed pressure drops were lower than what would have been predicted by using appropriate correlations.

In conclusion, this study does not claim to accurately capture the behavior of HCSGs, but rather aims to provide insights into the possibility of instabilities and into approaches to address them from a thermal-hydraulic perspective. Furthermore, it is imperative to consider these instabilities from a structural mechanics standpoint as well.

The development of a stability map in the Ishii-Zuber plane for the HCSGs was not pursued due to the absence of correlation in our model for pressure drops and heat transfer on both sides of the heat exchanger. This lack of correlations would have resulted in a map with potentially limited accuracy.

The adopted approach, although approximate, allowed to match fairly well the primary flow rate and core ΔT [14], as shown in Table 2. (data relative to case 1.1).

Table 2. Comparison of steady state parameters at reduced power

Power (%)	**Reference Primary flow (kg/s)**	**RELAP5-3D Primary flow (kg/s)**	**Reference Primary average temperature (° C)**	**RELAP5-3D Primary average temperature (° C)**	**Reference Core ΔT(° C)**	**RELAP5-3D Core ΔT(° C)**
15	280.2	300-305	284	279	17.6	15.9-16.2
50	443.7	438.5	284	282	36.9	36.3
75	521.6	519.9	284	283	46.9	45.7
100	587.0	588.4	284	286	55.4	53.0

5 A PRELIMINARY STUDY ON THE POTENTIAL POWER UPRATE OBTAINABLE BY SWITCHING FROM NATURAL TO FORCED CIRCULATION

5.1 Introduction

In the current investigation, we conducted a preliminary exploration into the potential enhancement of power output for the reference natural circulation iPWR through the implementation of forced circulation. It is well-established within the field that the flow rate achievable in a natural circulation system significantly lags behind that attainable through forced circulation mechanisms. This disparity notably compromises both the HTC and the temperature difference between the core's inlet and outlet. Consequently, the power output attainable in a reactor under natural circulation is notably inferior to that achievable with forced circulation. Our study therefore delved into the preliminary assessment of integrating primary pumps into our reference design.

5.2 Methodology

Central to the employed methodology was the utilization of a nodalization framework capable of accurately predicting steady-state parameters under natural circulation conditions. Leveraging this nodalization, we executed a procedure to enhance power output. This involved elevating the average linear heat generation rate of the hottest fuel rod to a maximum of 55 kW/m (17 kW/ft), with subsequent scaling of the total reactor power accordingly. The core thermal output power was therefore increased by almost a factor 5. Core axial and radial power distributions were maintained, as a first approximation, in line with the reference case.

Adjustments were made to the secondary and primary mass flow rates to ensure the production of superheated steam at the steam generator outlet and to maintain a reasonable subcooling level at the core outlet. Specifically, the secondary flow rate was determined through a simple energy balance calculation, while the speed of the primary pumps was regulated to achieve a core flow rate capable of providing a core ΔT approximately of 20° C. Increasing the superheat of the secondary steam ultimately results in a decrease in primary subcooling at the core outlet. In this analysis, emphasis was placed on prioritizing power extraction and core exit subcooling over thermodynamic efficiency. Although both primary and secondary pressures could have been increased to enhance overall efficiency, we chose to maintain these parameters at their reference levels for the current preliminary analysis. Regarding the calculation of the fuel cycle length, it was assumed that the maximum achievable burnup remains consistent with that of the natural circulation version. Therefore, to calculate it, we assume that it scales inversely with the power increase.

5.3 Pumps selection

Based on the reference design characteristics, the decision was made to incorporate primary pumps inspired to the ABWR's (Advanced Boiling Water Reactor) RIPs (Reactor Internal Pumps) [31]. This selection primarily stemmed from geometric considerations, particularly regarding the potential availability of free space within the downcomer/lower plenum region.

In fact, while iPWRs featuring primary pumps typically position them above the HCSGs, with the steam outlet piping exiting the vessel radially, our design differs. In our reference design, the steam generator piping enters the steam plenum along the reactor pressure vessel axis, occupying the upper part of the downcomer. Additionally, the flange allowing the detachment of the RPV's bottom and top parts for refueling is located below the HCSGs. Therefore, this placement of the pumps also would make sense from a maintenance standpoint. Furthermore, this positioning would enhance the NPSH available for the pumps, as they would be situated in a region with higher pressure and lower temperature compared to the downcomer upper region.

Four pumps with rated angular speed, torque, volumetric flow rate, and head matching those of the ABWR's RIPs were employed. Homologous curves from typical Westinghouse pumps were utilized due to the unavailability of the GE pumps curves. It's worth noting that this assumption could be debatable, especially given that Westinghouse pumps are centrifugal while the RIPs are mixed-flow pumps. The pumps' speed was adjusted using an integral controller to achieve the desired primary flow rate in steady state conditions.

5.4 Final considerations

The potential power increase for a natural circulation iPWR through the implementation of forced flow in the primary side has been preliminarily evaluated and the thermal power output has been increased by almost a factor 5. A snapshot of the comparison between the natural and the forced circulation versions of the reference iPWR is provided in Table 3.

Given the reduced dimensions of the core in the considered design and consequently the low achievable burnup, such a power uprate would result in a notably short fuel cycle, necessitating an assessment of its economic viability. One theoretically possible but challenging approach, considering political, regulatory, and supply chain constraints, would be to increase fuel enrichment to extend the fuel cycle length while maintaining the enhanced power output.

Furthermore, pumps features including design, location, maintenance, and cost should be carefully evaluated. Additionally, the lift force on the core and internals is significantly heightened compared to the natural circulation case, with core speeds increasing from 1 to 10 m/s. Moreover, the flow-induced vibrations on the steam generator tubes would require thorough assessment.

It's also worth noting that the impact of the power uprate on safety analysis has not been accounted for in this study. The elevated average temperature of the fuel under nominal conditions

in forced circulation may pose challenges for the currently employed emergency safety features and warrants further investigation.

Table 3. Comparison between relevant parameters for the reference i-PWR in natural and in forced circulation

#	**Reference iPWR in NC**	**Reference iPWR in FC**
Thermal power (MWth)	160	774
Maximum integrated linear heat generation rate (kW/m-kW/ft)	11.4-3.5	55-17
Average integrated linear heat generation rate (kW/m-kW/ft)	8.2-2.5	39.7-12.1
Primary flow (kg/s)	586	7070
Number of primary pumps	0	4
T hot primary (˚ C)	313	304
Core delta T (˚ C)	53	21
Subcooling at core exit (˚ C)	17	26
T hot secondary (˚ C)	311	249
Secondary side superheat (˚C)	69	6
Secondary pressure (bar)	34.5	35.5
Secondary flow (kg/s)	67	480
Core delta p (bar)	0.25	2.8
Fuel cycle length (months)	24	5

6 CONCLUSIONS

A RELAP5-3D nodalization for an iPWR operating in natural circulation has been developed and it has given satisfactory results in steady-state conditions.

Subsequently, several start-up scenarios have been analyzed and oscillations in the secondary side at low power conditions have arisen, raising concerns for instance about structural mechanics implications.

It's worth noting that the performed calculations on the instabilities are just scoping calculations and they do not claim to accurately predict frequency and amplitude of the instabilities: in fact, many simplifications are present in the model. First of all, appropriate correlations for pressure drops and heat transfer on both sides of HCSGs are not available in RELAP5-3D. In addition, the secondary side boundary conditions are both arbitrary and simplified. Also, the feedwater pumps have not been modelled, neither has the turbine. Furthermore, the bypass to the condenser for low power is neglected as well.

In conclusion, one of the benefits of switching to forced circulation, meaning the capability to increase the core power density and the reactor power output, has been preliminary assessed.

It is important to acknowledge that in the case of emerging designs like iPWRs, the quality of safety assessments falls short compared to those conducted for conventional PWRs or BWRs (Boiling Water Reactors). This discrepancy arises from limitations in experimental data available for ITFs (Integral Test Facilities), resulting in fewer analyzed scenarios and a smaller pool of system code benchmarks. It is crucial to clarify that this disparity does not imply inferior safety standards for new designs; rather, it underscores the need for enhanced validation, identification of thermal-hydraulic phenomena, and the need for increasing confidence in the quality of safety assessments. Additional investment is imperative to address these shortcomings.

HPC STANDARD ACKNOWLEDGMENT

This research made use of Idaho National Laboratory's High Performance Computing systems located at the Collaborative Computing Center and supported by the Office of Nuclear Energy of the U.S. Department of Energy and the Nuclear Science User Facilities under Contract No. DE-AC07-05ID14517.

REFERENCES

[1] INTERNATIONAL ATOMIC ENERGY AGENCY, "Status of Innovative Small and Medium Sized Reactor Design 2005", IAEA-TECDOC-1485, IAEA, Vienna (2006).

[2] INTERNATIONAL ATOMIC ENERGY AGENCY, "Design and Development Status of Small and Medium Reactor Systems 1995", IAEA-TECDOC-881, IAEA, Vienna (1996).

[3] F. D'Auria (2023) "Scaling, Passive Systems, and the AP-1000", Nuclear Science and Engineering, 197:5, 987-999, DOI: 10.1080/00295639.2023.2178874

[4] C.P. Marcel, H.F. Furci, D.F. Delmastro, V.P. Masson, "Phenomenology involved in self-pressurized, natural circulation, low thermo-dynamic quality, nuclear reactors: The thermal–hydraulics of the CAREM-25 reactor", Nuclear Engineering and Design 254 (2013) 218– 227

[5] H. Boado Magan, D. F. Delmastro, M. Markiewicz, E. Lopasso, F. Diez, M.

Giménez, A. Rauschert, S. Halpert, M. Chocrón, J.C. Dezzutti, H. Pirani, C. Balbi, "CAREM Prototype Construction and Licensing Status", IAEA-CN-164-5S01

[6] C.P. Marcel, F.M. Acu˜na, P.G. Zanocco, D.F. Delmastro, "Stability of self-pressurized, natural circulation, low thermo-dynamic quality, nuclear reactors: The stability performance of the CAREM-25 reactor", Nuclear Engineering and Design 265 (2013) 232– 243

[7] Octavio Fernando Bovati Davalos, Roberto Maturana, Federico Mezio, "Simulacion y analisis determinista de un reactor integrado de potencia con el codigo de planta RELAP: evaluaciones sobre el segundo sistema de extincion", proyecto integradoe de la carrera de ingenieria nuclear, 2017

[8] M. D. Carelli, L. Conway, L. Oriani, C. Lombardi, M. Ricotti, A. Barroso, J. Collado, L. Cinotti, M. Moraes, J. Kozuch, D. Grgic, H. Ninokata, R. Boroughs, D. Ingersoll, F. Oriolo, "THE DESIGN AND SAFETY FEATURES OF THE IRIS REACTOR", 11th International Conference on Nuclear Engineering

Tokyo, JAPAN, April 20-23, 2003, ICONE11- 36564

[9] Mario D. Carelli, Bojan Petrović, Nikola Čavlina, Davor Grgić "IRIS (International Reactor Innovative and Secure) – Design Overview and Deployment Prospects", International Conference Nuclear Energy for New Europe 2005, 132.9

[10] Status report 77 - System-Integrated Modular Advanced Reactor (SMART)

[11] A. Fakhrarei, F. Faghihi, M.A. Dast-Belaraki , "Theoretical study on the Passively Decay Heat Removal System and the primary loop flow rate of NuScale SMR", Annals of Nuclear Energy 161 (2021) 108420

[12] Jorge Sánchez Torrijos, César Queral, Javier Magán, "Analysis of Boron Dilution sequence in a NuScale Power Module using TRACE", 46 reunion annual Sociedad nuclear espanola

[13] A. Fakhraei, F. Faghihi, M. Amin-Mozafari, A. Sadegh-Noedoost, "Safety analysis of an advanced passively-cooled small modular reactor during station blackout scenarios and normal operation with RELAP5/SCDAP", Annals of Nuclear Energy 143 (2020) 107470

[14] NuScale Power LLC, "NuScale Standard Plant Design Certification Application", Rev. 5, 2020, U.S. Nuclear Regulatory Commission (NRC)

[15] The RELAP5-3D© Code Development Team, RELAP5-3D© CODE MANUAL VOLUME II: USER'S GUIDE AND INPUT REQUIREMENTS, INL/MIS-15-36723 Volume II Revision 4.4, 2018

[16] R. R. Schultz, RELAP5-3D© Code Manual Volume V: User's Guidelines, INL/MIS-15-36723 Volume V Revision 4.4, 2018

[17] Mascari, F., Vella, G., Woods, B.G., Welter, K., D'Auria F., "*Analysis of primary/containment coupling phenomena characterizing the MASLWR design during a SBLOCA scenario"*, Nuclear Power Plants, InTech, 2012.

[18] Y. Mori and W. NAKAYAMA, "Study on forced convective heat transfer in curved pipes" (1st report, laminar region), int. J. Heat Mass Transfer 8, 67-82 (1965).

[19] Y. Mori and W. NAKAYAMA, "Study on forced convective heat transfer in curved pipes" (2nd report, turbulent region), Int. J. Heat Mass Transfer 10, 37-59 (1967).

[20] Y. Mori and W. NAKAYAMA, "Study on forced convective heat transfer in curved pipes", (3rd report, theoretical analysis under the condition of uniform wall temperature and practical formulae), int. J. Heal Mass Transfer. Vol. IO, pp. 681-695. 1967

[21] D. G. Prabhanjan, G. S. V. Ragbavan and T. J. Kennic, "Comparison Of Heat Transfer Rates Between A Straight Tube Heat Exchanger And A Helically Coiled Heat Exchanger", 2022, lnt. Comm. Heat Mass Transfer Vol. 29. No. 2. pp. 185-191

[22] H. ITO, "Friction factors for turbulent flow in curved pipes", J. Bas. Engin 81D, 123-134 (1959)

[23] Lorenzo Santini, Andrea Cioncolini, Carlo Lombardi, Marco Ricotti, "Two-phase pressure drops in a helically coiled steam generator", 2007, International Journal of Heat and Mass Transfer 51 (2008) 4926–4939

[24] Lorenzo Santini, Andrea Cioncolini, Matthew T. Butel, Marco E. Ricotti, "Flow boiling heat transfer in a helically coiled steam generator for nuclear power applications", 2015, International Journal of Heat and Mass Transfer, 92 (2016) 91–99

[25] X.J. Chen, F.D. Zhou, "An investigation of flow pattern and frictional pressure drop characteristics of air–water two-phase flow in helical coils", in: Proceedings of the fourth Miami International Conference on Alternate Energy Sources, 1981, pp. 120–129.

[26] L. Zhao, L. Guo, B. Bai, Y. Hou, X. Zhang, "Convective boiling heat transfer and two-phase flow characteristics inside a small horizontal helically coiled tubing once-through steam generator", Int. J. Heat Mass Transfer 46 (2003) 4779–4788.

[27] L.J. Guo, Z. Feng, X. Chen, "An experimental investigation of the frictional pressure drop of steam-water two-phase flow in helical coils", Int. J. Heat Mass Transfer 44 (2001) 2601–2610.

[28] H.C. Unal, M.L. van Gasselt, P.M. van't Veerlat, "Dryout and twophase pressure drop in sodium heated helically coiled steam generator tubes at elevated pressures", Int. J. Heat Mass Transfer 24 (1981) 285– 298.

[29] A.E. Ruffell, "The application of heat transfer and pressure drop data to the design of helical coil once-through boilers", Symp. Multi-Phase Flow Systems, University of Strathclyde, Inst. Chem. Eng. Symp. Ser. 38 (1974) Paper 15.

[30] M. Ishii "Study On Flow Instabilities In Two-Phase Mixtures", Argonne National Laboratory, March 1976

[31] Status report 97 - Advanced Boiling Water Reactor (ABWR), https://aris.iaea.org/PDF/ABWR.pdf